Subunit stoichiometry of human Orai1 and Orai3 channels in closed and open states

Angelo Demuro[a,1], Aubin Penna[b], Olga Safrina[b], Andriy V. Yeromin[b], Anna Amcheslavsky[b], Michael D. Cahalan[b,c,1], and Ian Parker[a,b]

[a]Department of Neurobiology and Behavior, [b]Department of Physiology and Biophysics, and [c]Institute for Immunology, University of California, Irvine, CA 92697

Contributed by Michael D. Cahalan, September 9, 2011 (sent for review August 9, 2011)

We applied single-molecule photobleaching to investigate the stoichiometry of human Orai1 and Orai3 channels tagged with eGFP and expressed in mammalian cells. Orai1 was detected predominantly as dimers under resting conditions and as tetramers when coexpressed with C-STIM1 to activate Ca^{2+} influx. Orai1 was also found to be tetrameric when coexpressed with STIM1 and evaluated following fixation. We show that fixation rapidly causes release of Ca^{2+}, redistribution of STIM1 to the plasma membrane, and STIM1/Orai1 puncta formation, and may cause the channel to be in the activated state. Consistent with this possibility, Orai1 was found predominantly as a dimer when coexpressed with STIM1 in living cells under resting conditions. We further show that Orai3, like Orai1, is dimeric under resting conditions and is predominantly tetrameric when activated by C-STIM1. Interestingly, a dimeric Orai3 stoichiometry was found both before and during application of 2-aminoethyldiphenyl borate (2-APB) to activate a nonselective cation conductance in its STIM1-independent mode. We conclude that the human Orai1 and Orai3 channels undergo a dimer-to-tetramer transition to form a Ca^{2+}-selective pore during store-operated activation and that Orai3 forms a dimeric nonselective cation pore upon activation by 2-APB.

calcium signaling | Ca^{2+} release-activated Ca^{2+}

In many cell types, store-operated Ca^{2+} entry (SOCE) is mediated through activation of Ca^{2+} release-activated Ca^{2+} (CRAC) channels and plays a pivotal role in intracellular Ca^{2+} homeostasis (1). Recent studies have revealed that stromal interaction molecule (STIM) and Orai proteins, are both required for the activation of CRAC currents (2–7). Following the identification of *Drosophila* Stim and Orai by RNAi screening, two homologs for human STIM (STIM1 and STIM2) and three homologs for human Orai (Orai1, Orai2, and Orai3) were identified and are present in various tissues. In particular, STIM1 and Orai1 play a critical role in the initiation of the immune response (8).

Within the past 5 y, considerable progress has been made toward identifying the molecular mechanisms by which Orai and STIM interact following endoplasmic reticulum (ER) Ca^{2+} store depletion (2). STIM proteins are strategically localized in the ER membrane and function as sensors of Ca^{2+} levels within the ER lumen. In response to ER Ca^{2+} store depletion, STIM proteins translocate to junctions adjacent to the plasma membrane (PM) to activate Orai, the pore-forming component of the CRAC channel located in the PM. Functional domains of STIM proteins have been identified: the N-terminal EF hand situated in the ER lumen, which mediates Ca^{2+} sensing; the sterile alpha motif (SAM) domain, which mediates oligomerization of STIM proteins following Ca^{2+} unbinding from the EF hand; the membrane-proximal coiled-coil domain in the cytosol, which allows STIM proteins to dimerize in the resting state; and the distal coiled-coil domain, which interacts with Orai proteins. Truncated C-terminal STIM proteins, including the proximal and distal coiled-coil domains, are able to activate Ca^{2+} influx through the corresponding Orai channels: C-STIM1 interacting with Orai1 or *Drosophila* C-Stim interacting with *Drosophila* Orai (9–14). Further studies delineated a smaller portion of the distal coiled-coil region as essential for interaction with and activation of Orai1 (15–18). A direct binding interaction between one of these activating peptides and purified Orai1 has been demonstrated (17), and recombinant STIM1 has been shown to activate Orai1 in vesicles isolated from yeast cells (19).

Despite progress in identifying important functional domains of STIM and Orai proteins, the gating mechanism and pore stoichiometry of Orai remain uncertain. Measurement of Ca^{2+} current through expressed tandem Orai1 multimers suggested that Orai1 monomers associate in a tetrameric complex in the active state (20, 21), whereas initial biochemical experiments pointed to a dimeric Orai complex in both resting and active states (22). Three groups investigated the stoichiometry of Orai1 and Orai in the resting and activated states by using single-molecule imaging (10, 12, 23). In this method, proteins are tagged with eGFP and expressed at a sufficiently low density to permit visualization of single molecular complexes. Using total internal reflection fluorescence (TIRF) microscopy under bright illumination, the fluorescence decays in a stepwise manner as individual eGFP molecules bleach; by counting the number of photobleach steps (24), or by statistical analysis of fluorescence intensity distributions (23), the number of subunits per complex can be deduced. All papers that applied this method (10, 12, 24) agree on the tetrameric subunit composition of Orai (or Orai1) in the active state. However, different conclusions were proposed for resting conditions. Using *Drosophila* Orai and C-Stim expressed in *Xenopus* oocytes and in *Drosophila* S2 cells, a convergence of biochemical and single-molecule photobleaching techniques indicated that Orai is predominantly a dimer when expressed alone and a tetramer when coexpressed with C-Stim (12). In contrast, other groups found that human Orai1 is predominantly tetrameric in both basal and activated states (10, 23), raising the possibility of different activation mechanisms between *Drosophila* and human Orai1, or differences in experimental procedures.

To help resolve the stoichiometry of Orai1 in the resting and activated states, we monitored single-molecule photobleaching steps of human eGFP–Orai1 when expressed alone, expressed together with the activator C-STIM1, or expressed together with full-length STIM1 in HEK cells. For experiments involving coexpressed eGFP–Orai1 and STIM1, we used transfection and fixation conditions comparable to those used by Ji et al. (10) and compared these results with those obtained in living HEK cells under resting conditions.

Author contributions: A.D., A.P., M.D.C., and I.P. designed research; A.D., A.P., O.S., and A.V.Y. performed research; A.A. contributed new reagents/analytic tools; and A.D., A.P., A.V.Y., M.D.C., and I.P. wrote the paper.

The authors declare no conflict of interest.

[1]To whom correspondence may be addressed. E-mail: ademuro@uci.edu or mcahalan@uci.edu.

This article contains supporting information online at www.pnas.org/lookup/suppl/doi:10.1073/pnas.1114814108/-/DCSupplemental.

In addition, we examined the subunit stoichiometry of the Orai3 homolog under resting conditions and during two very distinct activating conditions. Orai3, like Orai1, can be activated by store depletion via STIM1 to form a Ca^{2+}-selective CRAC-like current with similar biophysical properties (14). The compound 2-aminoethyldiphenyl borate (2-APB) has complex actions on native CRAC current, potentiating at low concentrations (1–10 μM) and strongly inhibiting at higher concentrations (25, 26). However, Orai3 can also be activated in a store- and STIM1-independent manner by 2-APB (14, 27, 28). At high concentrations (>20 μM), 2-APB activates Orai3 to form a Ca^{2+}-permeable but rather nonselective cation current with very distinct biophysical properties (14). To compare the subunit stoichiometry of Orai3 under these two activating conditions, we investigated photobleaching of eGFP–Orai3 when expressed alone, when expressed together with C-STIM1 to activate a Ca^{2+}-selective conductance, or in the presence of 2-APB to activate the store-independent nonselective cation conductance.

Results

Functional Expression of Fluorescent-Tagged Orai Constructs. We sought to investigate the subunit stoichiometry of Orai1 and Orai3 in HEK cells under resting and activated conditions, using TIRF microscopy to count photobleaching steps in cells expressing eGFP-tagged Orai1 or Orai3 alone or together with C-STIM1, the cytosolic activator portion of STIM1. Constructs and methods are shown schematically in Fig. S1.

We first determined the conditions to achieve the low level of eGFP–Orai1 and eGFP–Orai3 expression necessary to discern individual molecules and tested for function using Ca^{2+} imaging. Within 3–5 h of transfection of eGFP–Orai1 together with C-STIM1, cells showed constitutive calcium influx that was inhibited by 50 μM of 2-APB, consistent with functional activation of the Orai1 channels by C-STIM1 (Fig. 1 *A* and *B*). Protein expression was barely detectable by Western blot at this early time point, but strong expression of both proteins was detected 16 h following transfection, confirming efficient production of fusion proteins at the expected sizes (Fig. S2). Constitutive Ca^{2+} influx was absent in cells transfected with eGFP–Orai1 alone and when a non-conducting eGFP-tagged Orai1 pore mutant (E106A) was coexpressed together with C-STIM1 (Fig. 1 *A* and *B*). Constitutive Ca^{2+} influx through wild-type Orai3 channels was also observed when C-STIM1 was coexpressed (Fig. 1 *C* and *D*). Mutation of the critical pore glutamate residue to glutamine (E81Q), shown previously to inhibit 2-APB- or STIM1-induced Orai3 channel activity, abolished this activation. Moreover, addition of 2-APB resulted in a modest potentiation of the Ca^{2+} signal when wild-type Orai3 was coexpressed with C-STIM1, and it induced a sizeable Ca^{2+} influx when wild-type Orai3 alone was expressed, as described previously (14).

To further characterize the functional expression of Orai3 channels, we used whole-cell recording to monitor properties of a nonselective conductance activated by 2-APB in eGFP–Orai3–transfected cells (Fig. S3). We observed fluctuations in current and evaluated the single-channel current by noise variance analysis. Dividing current variance by mean currents provided an estimate of single channel chord conductance (0.79 ± 0.13 pS), substantially larger than that of native STIM1-operated CRAC channels (21–36 fS) (26, 29). The average number of channels per cell was 1,953 ± 641, corresponding to an average channel density of 1.2 ± 0.4 channels per μm^2 of surface membrane area. Measurements were made 3 to 5 h following transfection but from selected cells with brighter GFP fluorescence, so that these values likely represent a higher level of expression than in cells chosen for photobleaching experiments.

Taken together with Ca^{2+} imaging experiments in Fig. 1, our results demonstrate functional expression of eGFP-tagged Orai1 and Orai3 proteins within 3 to 5 h following transfection.

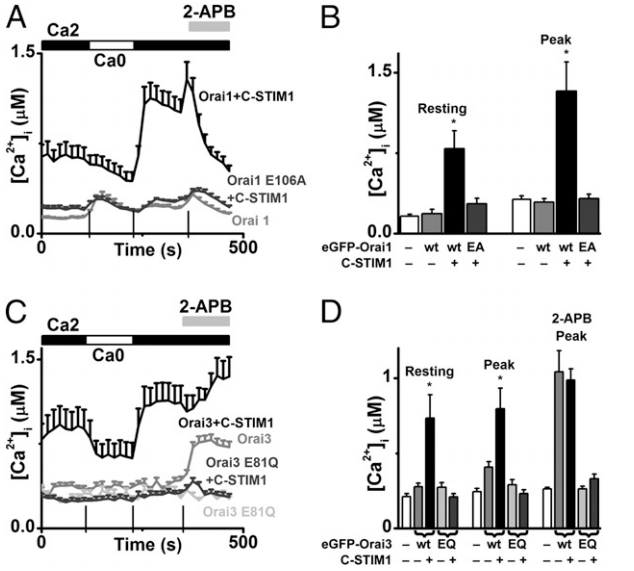

Fig. 1. Functional expression of Orai1 and Orai3. (*A*) Fura-2 ratiometric Ca^{2+} measurements in response to removal and readdition of extracellular Ca^{2+}, followed by application of 50 μM of 2-APB. Cells were transfected with eGFP–Orai1 alone (light gray), a 1:5 ratio of eGFP–Orai1/C-STIM1 (black), or eGFP–Orai1 E106A (a dominant-negative nonconducting pore mutant) together with C-STIM1 (dark gray). Measurements were made 3 to 5 h after transfection. Traces show means and SEM from one representative experiment of six experiments; each experiment typically included >50 cells. (*B*) Initial basal cytosolic $[Ca^{2+}]$ levels when bathed in solution containing 2 mM Ca^{2+} (*Left*), and the increase in cytosolic $[Ca^{2+}]$ resulting from readmission of 2 mM Ca^{2+} after bathing in zero $[Ca^{2+}]$ solution (*Right*). Error bars indicate SEM from six experiments; $^*P < 0.05$ compared with mock-transfected cells (open bars). (*C*) Fura-2 Ca^{2+} measurements in eGFP–Orai3-transfected cells in response to removal and readdition of extracellular Ca^{2+}, followed by application of 50 μM of 2-APB. Black trace is from cells transfected with eGFP–Orai3 (WT) together with C-STIM1, gray trace from cells transfected with eGFP–Orai3 alone, light gray trace from cells transfected with an eGFP-tagged dominant-negative mutant (E81Q, EQ) of Orai3, and dark gray trace from cells transfected with eGFP–Orai3 E81Q together with C-STIM1. (*D*) Analysis of Ca^{2+} measurements from experiments similar to *C*, showing resting $[Ca^{2+}]$ levels, peak $[Ca^{2+}]$ levels following Ca^{2+} readdition, and peak $[Ca^{2+}]$ levels following application of 2-APB. Error bars indicate 1 SEM from 6 to 12 experiments.

eGFP–Orai1 Is a Dimer at Rest and a Tetramer When Activated by C-STIM1. HEK cells expressing eGFP–Orai1 alone, or together with C-STIM1 to cause constitutive activation of Orai1 without puncta formation, were fixed with paraformaldehyde (PFA) 3 h after transfection for subsequent imaging by TIRF microscopy. Continuous exposure to laser excitation (488 nm: ~600 W cm^{-2}) induced a stochastic, stepwise loss of fluorescence from individual spots over several seconds, characteristic of photobleaching of single eGFP molecules (Fig. 2 *A* and *B*). By counting the number of bleaching steps at each spot we could thus estimate the number of Orai1 subunits (each tagged with a single eGFP) present in the spot. We interpret this to reflect the subunit stoichiometry of individual Orai multimers, because the sparse distribution of spots minimized the possibility of chance overlap of two spots.

Analysis of the bleaching steps for cells expressing human eGFP–Orai1 alone showed that the great majority of the selected bright spots bleached in one or two steps, whereas three- and four-step bleaching patterns were observed only infrequently (Fig. 2*C*, open bars; see also Movie S1). This suggests that Orai1 was present predominantly as dimers, given that a proportion of single-step bleaching events are expected to arise even from dimers, owing to the existence of dark eGFP states and failures to resolve separate steps when two eGFP molecules happen by

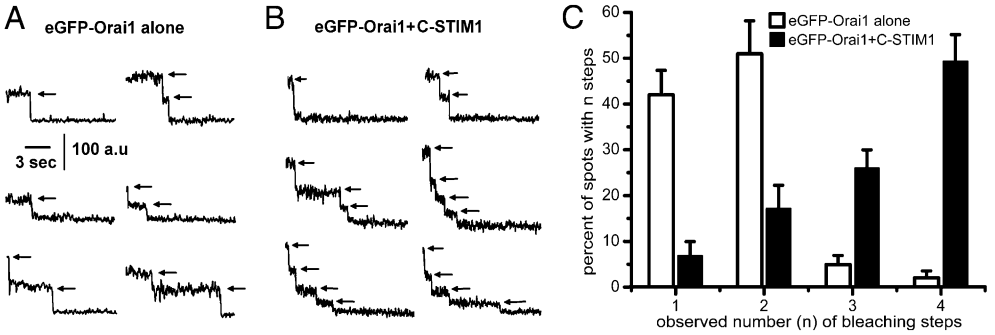

Fig. 2. Subunit stoichiometry of Orai1 at rest and when activated by coexpression of C-STIM1. (*A* and *B*) Representative traces showing single-spot bleaching steps in fixed HEK cells expressing, respectively, eGFP–Orai1 alone, or eGFP–Orai1 plus C-STIM1. Arrows indicate visually identified bleaching steps. Fluorescence is expressed in arbitrary units (AU). (*C*) Histograms showing percentages of spots showing one, two, three, or four bleaching steps in fixed cells expressing eGFP–Orai1 alone (open bars; 146 spots, 14 cells) or eGFP–Orai1 plus C-STIM1 (filled bars; 237 spots, 14 cells). Comparison of the bleaching step distributions for eGFP–Orai1 with and without C-STIM1 yielded $P < 0.0001$ (χ^2 test).

chance to bleach at nearly the same time. These results are consistent with our previous findings obtained with *Drosophila* Orai expressed in *Xenopus* oocytes (12) and suggest a predominantly dimeric subunit composition of Orai1 when expressed alone and in a nonconducting state.

In contrast, coexpression of eGFP–Orai1 with C-STIM1 resulted in a marked shift in the distribution of photobleaching patterns, with the majority of spots exhibiting three or four steps (Fig. 2*C*, filled bars; see also Movie S2). This again is in agreement with our previous result with *Drosophila* Orai, suggesting that our proposed model in which Orai dimers are induced to dimerize by C-STIM (12) can be extended to human Orai1.

eGFP–Orai1 Coexpressed with STIM1 Is a Dimer in Living Cells, but Is Detected as a Tetramer After Fixation. Although our finding of a tetrameric active state of Orai1 is in agreement with results on *Drosophila* Orai and with other studies on Orai1 (10, 12, 20, 21), our finding of a predominantly dimeric resting state differs from the tetrameric structure proposed by Ji et al. (10), who also used single-molecule photobleaching to elucidate the stoichiometry of Orai1. To investigate this discrepancy, we attempted to replicate the conditions described by Ji et al. by imaging fixed HEK cells expressing the C-terminal tagged Orai1–eGFP construct used by those authors together with STIM1 at a respective DNA ratio of 1:5. We compared photobleaching steps in these fixed cells with those in living cells before fixation. Our results in fixed cells (Fig. 3*A*, gray bars) are in accord with the data of Ji et al. (10), with most spots showing four bleaching steps consistent with an Orai1 tetramer. On the other hand, fixed cells expressing only Orai1–eGFP showed predominantly one or two photobleaching steps (Fig. 3*A*, open bars), similar to results obtained with our N-terminal–tagged eGFP–Orai1 construct (Fig. 2*C*, open bars). Moreover, measurements of stationary spots in unstimulated living cells expressing STIM1 together with either eGFP–Orai1 or mCherry–Orai1 (Fig. 3*A*, black and hatched bars, respectively; see also Movie S3) also showed predominantly one or two photobleaching steps, consistent with a dimeric state of Orai1 in the absence of ER Ca^{2+} store depletion.

These results suggested that the fixation process may artifactually trigger dimerization of Orai1 dimers as a result of mobilization of STIM1, perhaps because fixation induces Ca^{2+} store depletion. We thus performed fura-2 imaging of cytosolic Ca^{2+} during the process of fixation in living cells expressing eGFP–Orai1 and STIM1 at levels comparable to those used in photobleaching experiments. Addition of PFA in the absence of extracellular Ca^{2+} indeed resulted in an elevation of cytosolic Ca^{2+}, which was sustained in contrast to the transient elevation seen following addition of ionomycin or thapsigargin (Fig. 3*B*). We postulate that PFA crosses the plasma membrane and induces rapid release of Ca^{2+} from the ER, resulting in an elevation of cytosolic Ca^{2+} that is sustained because the plasma membrane Ca^{2+} transporters become inhibited by the fixative. Concordant with the notion that PFA induces ER Ca^{2+} store depletion, we also observed redistribution of STIM1 and Orai1 into puncta during fixation (Fig. 3 *C–F*).

Collectively, our results suggest that the resting state of Orai1 is a dimer, even when STIM1 is coexpressed, and that the tetrameric pattern of photobleaching steps seen in fixed cells coexpressing STIM1 may result artifactually from ER Ca^{2+} store depletion and rapid mobilization of STIM1 to the plasma membrane before protein fixation is complete.

Stoichiometry of eGFP–Orai3 in the Basal and Active States. Orai3 forms conducting ion channels in response to two very different activation stimuli. As is the case for Orai1, Orai3 can be opened by physiological store depletion via STIM1 to form a Ca^{2+}-selective channel. In addition, Orai3 can be activated by 2-APB in a STIM1-independent manner to form a channel that has distinct electrophysiological properties (current/voltage relationship) (Fig. S3*B*) and ion selectivity (14, 27, 28). This prompted us to investigate the stoichiometry of Orai3 channels under these two different activating conditions.

Figure 4 *A* to *C* shows representative examples of single-molecule bleaching records obtained in fixed cells expressing eGFP–Orai3 alone under resting conditions and after application of 2-APB, and when Orai3 was expressed together with C-STIM1. Analogous to our observations with Orai1, expression of eGFP–Orai3 alone resulted in predominantly one- and two-step bleaching patterns under basal conditions (Fig. 4*D*, open bars), but mostly as three- and four-step bleaching patterns when coexpressed with C-STIM1 (Fig. 4*D*, gray bars). On the other hand, cells expressing only eGFP–Orai3 that were exposed to 2-APB before fixation showed a distribution of bleaching steps closely similar to that observed without 2-APB, with a predominance of one- and two-step patterns (Fig. 4*D*, black bars). These results indicate a predominantly dimeric state for Orai3 at rest or when activated by 2-APB, and a predominantly tetrameric channel when activated by C-STIM1.

Discussion

We had previously shown by biochemical analysis and single molecule imaging that *Drosophila* Orai undergoes a dimer-to-tetramer transition when coexpressed with C-STIM to activate Ca^{2+} influx (12). We now extend those findings to the stoichiometry of the mammalian homologs Orai1 and Orai3 in the resting and open states. Measurements were obtained by

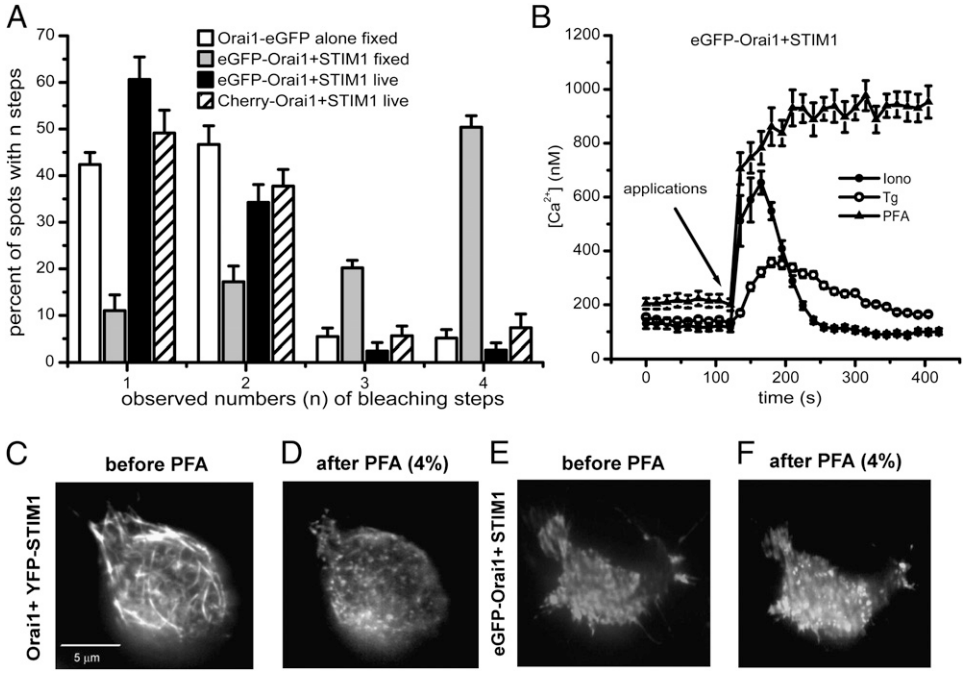

Fig. 3. Fixation evokes release of intracellular Ca^{2+}, and in cells expressing STIM1 results in redistribution of Orai1 and STIM1 and shifts bleaching patterns of eGFP–Orai1 from primarily dimeric to tetrameric. (*A*) Histograms showing percentages of spots showing one, two, three, or four bleaching steps in fixed HEK cells expressing Orai1–eGFP alone (open bars; 185 spots, 16 cells), in fixed cells expressing eGFP–Orai1 + full-length STIM1 (gray bars; 114 spots, 13 cells); and in living cells expressing eGFP–Orai1 + full-length STIM1 (black bars; 90 spots, 7 cells), or mCherry–Orai1 + full-length STIM1 (hatched bars; 137 spots, 11 cells). Comparison of bleaching step distributions for eGFP–Orai1 + STIM1-expressing cells before and after fixation yielded $P < 0.0001$ (χ^2 test). (*B*) Fura-2 Ca^{2+} measurements in HEK cells expressing eGFP–Orai1 + STIM1 in the absence of extracellular Ca^{2+}. Arrow indicates application times of 5 μM ionomycin (filled circles), 1 μM thapsigargin (open circles), and 4% PFA (triangles). (*C–F*) PFA fixation triggers redistribution of YFP–STIM1 and eGFP–Orai1. (*C*) A single cell expressing Orai1 + YFP–STIM1 before PFA application. (*D*) The same cell, imaged after treatment with Ca^{2+}-free PBS solution containing 4% PFA (pH 7.4) at 23 °C for 5 min, and then washed with fresh PBS for 30 min. (*E* and *F*) Corresponding images before and after PFA treatment of a cell expressing eGFP–Orai1 + STIM1. The brightness and contrast settings in *D* and *F* were adjusted compared with the prefixation images in *C* and *E* to compensate for fluorescence quenching induced by PFA.

counting single-molecule photobleaching steps of eGFP-tagged Orai1 and Orai3 expressed in HEK cells; and in most experiments, we examined cells after PFA fixation so as to "freeze" protein expression at appropriately low densities and to circumvent problems of movement in live cells.

To resolve the stoichiometry of Orai1 and Orai3 in the store-operated open state we coexpressed C-STIM1 to evoke constitutive channel activation (12, 13). This approach obviates the requirement for Ca^{2+} store depletion and consequent formation of dense puncta, which confound observation of individual single-molecule fluorescent spots. However, a possible caveat is that newly synthesized Orai molecules will be chronically exposed to C-STIM1 and may, for example, multimerize with one another before insertion into the PM. In agreement with our findings on *Drosophila* Orai (12), we find that mammalian Orai1 and Orai3 predominantly show three- and four-step bleaching patterns when activated by C-STIM1. Given that some eGFP molecules may be in a dark state, and that bleaching steps will be undercounted owing to instances when two eGFP molecules randomly bleach at nearly the same time, we conclude that both Orai1 and Orai3 are predominantly tetramers when in the physiological open state. A tetrameric functional channel was also reported for Orai1 in functional studies on tandem constructs (20, 21) and by imaging studies at the single-molecule level (10, 23).

On the other hand, our results show that both Orai1 and Orai3 display mostly one- and two-step bleaching patterns under resting conditions without store depletion. A concern is whether the true stoichiometry may by undercounted if the fluorescently tagged Orai monomers were to associate together with untagged native Orai in higher order multimers. We consider this unlikely. HEK cells display very small native CRAC currents (30, 31), and the GFP-tagged Orai subunits were expressed using a strong CMV promoter so they would be expected to be synthesized at a greater rate than the endogenous Orai monomers; the observed distribution of bleaching steps does not fit a model in which tagged monomers associate randomly into tetramers with any proportion of untagged native monomers, and, in particular, it is difficult to envisage how C-STIM1 could selectively promote the association of tagged, exogenous Orai monomers given that expression levels (densities of fluorescent spots) were similar with and without C-STIM coexpression. Moreover, our results with mammalian Orai1 and Orai3 are consistent with single-molecule photobleaching and biochemical experiments on *Drosophila* Orai (12) in indicating a predominantly dimeric composition when the channel is expected to be closed.

This conclusion differs from a report by Ji et al. (10), who describe a resting tetrameric Orai1 stoichiometry in fixed cells. We believe that the discrepancy may be explained because Ji et al. coexpressed Orai1 together with an excess of full-length STIM1, whereas we expressed only Orai1. Indeed, we were able to confirm the finding of predominantly three- and four-step bleaching steps in fixed cells prepared using procedures as described by Ji et al. We show that fixation with PFA appears to promote Ca^{2+} release, redistribution of STIM1 to the plasma membrane, and STIM1/Orai1 puncta formation, which may account for the tetrameric Orai1 stoichiometry reported by Ji et al. (10) under what were previously thought to be "resting conditions" in fixed cells. Moreover, our finding that eGFP-tagged Orai1 spots in living cells under resting conditions show predominantly one- and two-step bleaching steps, even when coex-

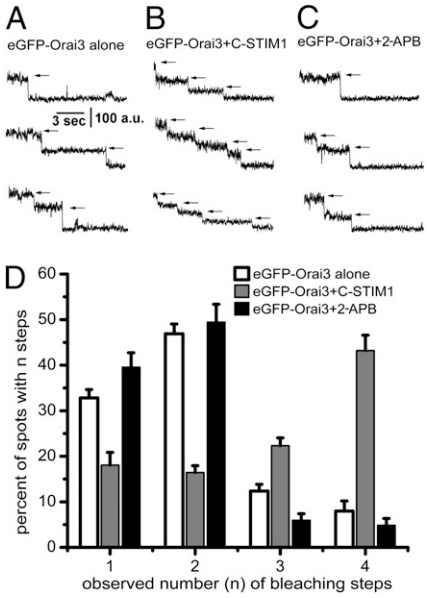

Fig. 4. Subunit stoichiometry of eGFP–Orai3 alone and when activated by C-STIM1 or by 2-APB. (*A*–*C*) Representative traces showing bleaching steps from experiment in fixed cells expressing: (*A*) eGFP–Orai3 alone, (*B*) eGFP–Orai3 + C-STIM1, or (*C*) eGFP–Orai3 alone following application of 100 μM of 2-ABP. Arrows indicate visually identified bleaching steps. (*D*) Histograms showing percentages of spots showing one, two, three, or four bleaching steps in HEK cells expressing: eGFP–Orai3 alone (white bars, 287 spots, 19 cells), eGFP–Orai3 + C-STIM1 (gray bars; 257 spots, 16 cells), or eGFP–Orai3 following application of 100 μM of 2-APB (black bars; 235 spots, 23 cells). Comparison of bleaching step distributions for eGFP–Orai3 and eGFP–Orai3 +2-APB gave no significant difference ($P = 0.127$; χ^2 test).

pressed with STIM1, further supports the notion of a dimeric resting state.

The stoichiometry of Orai1 has also been investigated by Madl et al. (23) using two different techniques: FRET measurements on fluorescently labeled tandem repeat constructs and brightness analysis of motile fluorescently labeled Orai1 channels in living HEK cells. Both methods indicated a tetrameric subunit composition of Orai1 under resting as well as activated conditions. Reasons for the discrepancy with our conclusion of a dimeric resting state of Orai1 are not clear. Among the methodological differences, Madl et al. (23) applied brightness analysis to the population of motile molecules that diffused into a previously bleached region of membrane of living cells, whereas our data are derived primarily from fixed cells; and in the case of live cells, we analyzed only relatively stationary molecules. Furthermore, the motility of the Orai1 molecules precluded Madl et al. (23) from directly counting bleaching steps, and instead they based their conclusions on analysis of subtle differences in distributions of fluorescent spot intensities. That analysis assumes that the brightness of a fluorescence spot is directly proportional to the number of fluorescent protein molecules present (23), but there are indications that a simple linear relationship may not apply. Specifically, our data (e.g., Figs. 2 and 3) and several published reports (10, 24, 32) show that the magnitudes of successive bleaching steps recorded from multimeric-tagged proteins differ appreciably, suggesting that individual fluorophores may not emit independently; and Ding et al. (32) describe that measurements of the relative fluorescence intensity of a spot do not strictly correlate with the number of fluorophores within the spot. Further differences include expression level and temperature; Madl et al. (23) imaged at 37 °C, which may enhance interaction with endogenous STIM (33).

We also investigated the stoichiometry of Orai3 channels in the resting state and during channel activation by two different modalities. Like Orai1, we find that human Orai3 is predominantly a dimer at rest and a tetramer when coexpressed with C-STIM1 to mimic physiological activation. However, our results indicate that Orai3 remains dimeric when activated by 2-APB. Channel dimers are unusual, but not unprecedented. For example, single-molecule photobleaching experiments complemented by functional studies using tandem dimer constructs have shown that the voltage-gated proton channel HV1 forms dimers in which each monomer has the capacity to conduct protons (34). Our results thus suggest two very different mechanisms by which 2-APB activation and STIM1 activation form the conducting pore, despite the fact that both conducting states of Orai3 are blocked by glutamine substitution of an essential glutamate residue (position 81 in the first transmembrane segment, homologous to the critical E106 in Orai1; Fig. 1 and ref. 14). We propose that channel opening by 2-APB requires only a ligand-induced conformational change in the dimer, whereas STIM1 activation first requires STIM1 translocation followed by STIM1-induced dimerization of Orai1 dimers. The contrasting mechanisms and stoichiometries likely underlie differences between the rapid exponential activation kinetics upon addition of 2-APB, in comparison with the slower and delayed activation kinetics following store depletion (7, 14).

Taken together, the present results with Orai1 and Orai3 and our previous study on *Drosophila* Orai (12) suggest that STIM protein dimers bring nonconducting Orai dimers together to form the conducting tetrameric channel. Similar to many ion channels, the physiological conducting state of both Orai1 and Orai3 is a tetramer. However, what appears unprecedented about STIM-operated Orai channel activation is the change in stoichiometry induced by the activator protein in forming the conducting tetrameric channel. The fact that STIM1 and *Drosophila* Stim serve as diffusion traps to aggregate Orai subunits into puncta is well documented (12, 35, 36). The activator STIM proteins are dimeric, as shown using single-molecule photobleaching by Ji et al. (10). In this respect, the STIM proteins function in a manner analogous to antibody- or ligand-induced dimerization of many tyrosine-kinase–linked receptors, the difference being that STIM proteins operate from the cytosolic side of the membrane. In the fully active state, an Orai1 tetramer may have as many as eight STIM1 molecules in effect cross-linked, as implied by self-activating STIM1/Orai1 concatemer studies (37) and by a quantitative fluorescence ratio imaging method (38).

Our results on Orai1 and Orai3 are summarized in Fig. S4. For Orai1 and Orai3, we validate that STIM proteins induce dimerization of mammalian Orai protein dimers to form the active tetrameric channel, as previously shown for *Drosophila* Orai (12) and further show that the Orai3 protein can function as a Ca^{2+} permeable channel either as a STIM1-operated tetramer or as a 2-APB–activated dimer.

Materials and Methods

Cell Culture and Transfection. Human embryonic kidney HEK293 cells (ATCC) were maintained and propagated as recommended by the ATCC. Cell suspensions were transfected using Lipofectamine 2000 (Invitrogen) reagents, without or with STIM1 constructs and the different Orai vectors mixed in a 1:5 weight ratio [0.5 μg and 2.5 μg of the Orai and STIM1 or C-STIM1 constructs, respectively, plus 0.5 μg of eGFP-expressing vector (pmaxGFP; Lonza) for the calcium imaging experiments], and plated on 0.1 mg/mL poly-L-lysine–coated glass bottom 35-mm dishes (Matek) for single-molecule photobleaching experiments or home-made glass bottom chambers for single-cell $[Ca^{2+}]_i$ imaging or whole-cell recording. Following transfection, cells were used or fixed at ~3 h for TIRF single-molecule imaging, and used at 3 to 5 h for single-cell $[Ca^{2+}]_i$ imaging, and 12 to 16 h for Western blotting.

Western Blotting. Western blotting of transfected HEK cells was performed as described in *SI Materials and Methods*.

Single-Cell $[Ca^{2+}]_i$ Imaging. Ratiometric fura-2 $[Ca^{2+}]_i$ imaging in transfected HEK cells was performed as described (5, 39), using solutions described in *SI Materials and Methods*.

Whole-Cell Recording. Whole-cell recordings were done on transfected HEK 293 cells as described, using external and pipette solutions described in *SI Materials and Methods*.

Single-Molecule Photobleaching. Live HEK cells were imaged in Ca^{2+}-containing PBS 3 h after transfection. For fixed cell experiments, cells were treated at this time with Ca^{2+}-free PBS containing 4% PFA (Electron Microscopy Sciences) for 15 min at room temperature, rinsed extensively, and maintained in PBS solution for 2–48 h before imaging.

TIRF microscopy of single fluorescent protein-tagged Orai1 and Orai3 molecules was accomplished using a home-built system (40) based on an Olympus IX70 microscope equipped with a 60×, NA 1.45 TIRF objective. Cells were imaged on the cover glass forming the base of the recording chamber and fluorescently tagged molecules lying within the ∼100-nm evanescent field were excited by TIRF using, respectively, 488 nm and 532 nm lasers for eGFP and mCherry. Images (128 × 128 pixel; 1 pixel = 0.33 μm) were acquired at 10 frames/s^{-1} by a Cascade 128$^+$ electron multiplying CCD camera (Roper Scientific). The resulting image stacks (up to 4,000 frames; 400 s) were processed in MetaMorph (Molecular Devices) by subtracting a heavily smoothed (6 × 6 pixel) copy of each frame so as to correct for time-dependent changes resulting from background bleaching, laser fluctuations, and drift in camera offset level. A two-stage process was used to select and analyze fluorescence spots. First, 3 × 3 pixel regions of interest were centered around spots that were present in the first few frames after opening the laser shutter, and which had a spatial width of no more than 3 pixels. Measurements of maximal intensity within the regions of interest were then exported to Origin (OriginLab) for visual inspection. Bleaching steps were identified as abrupt (≤ 2 frames) decrements in fluorescence between dwell states during which the intensity fluctuated within the noise level around a stable value for ≥ 3 frames. Traces that did not show clear bleaching steps (typically about one-third of those initially selected) were rejected. The percentages of spots showing one, two, three, or four bleaching steps are presented as means ± SEM of numbers of cells examined. To enhance display, traces in Figs. 2 and 4 were further smoothed using a 4-point running average. Bleaching steps in live-cell experiments were determined from a subset of fluorescent spots that showed low motility (<1 μm displacement before full bleaching), and measurements were made of maximum intensity within regions of interest chosen to encompass any movement of the spots.

ACKNOWLEDGMENTS. We thank Dr. L. Forrest for assistance with cell culture, and Liangyi Chen and Tao Xo for providing the Orai1–eGFP construct. This research was supported by National Institutes of Health Grants GM-48071 (to I.P.) and NS-14609 (to M.D.C.), and by a postdoctoral fellowship from the Hewitt Foundation (to A.P.).

1. Parekh AB, Putney JW, Jr. (2005) Store-operated calcium channels. *Physiol Rev* 85: 757–810.
2. Cahalan MD (2009) STIMulating store-operated Ca^{2+} entry. *Nat Cell Biol* 11:669–677.
3. Feske S, et al. (2006) A mutation in Orai1 causes immune deficiency by abrogating CRAC channel function. *Nature* 441:179–185.
4. Liou J, et al. (2005) STIM is a Ca^{2+} sensor essential for Ca^{2+}-store-depletion-triggered Ca^{2+} influx. *Curr Biol* 15:1235–1241.
5. Roos J, et al. (2005) STIM1, an essential and conserved component of store-operated Ca^{2+} channel function. *J Cell Biol* 169:435–445.
6. Vig M, et al. (2006) CRACM1 is a plasma membrane protein essential for store-operated Ca^{2+} entry. *Science* 312:1220–1223.
7. Zhang SL, et al. (2006) Genome-wide RNAi screen of Ca^{2+} influx identifies genes that regulate Ca^{2+} release-activated Ca^{2+} channel activity. *Proc Natl Acad Sci USA* 103: 9357–9362.
8. Cahalan MD, Chandy KG (2009) The functional network of ion channels in T lymphocytes. *Immunol Rev* 231:59–87.
9. Huang GN, et al. (2006) STIM1 carboxyl-terminus activates native SOC, I(crac) and TRPC1 channels. *Nat Cell Biol* 8:1003–1010.
10. Ji W, et al. (2008) Functional stoichiometry of the unitary calcium-release–activated calcium channel. *Proc Natl Acad Sci USA* 105:13668–13673.
11. Muik M, et al. (2008) Dynamic coupling of the putative coiled-coil domain of ORAI1 with STIM1 mediates ORAI1 channel activation. *J Biol Chem* 283:8014–8022.
12. Penna A, et al. (2008) The CRAC channel consists of a tetramer formed by Stim-induced dimerization of Orai dimers. *Nature* 456:116–120.
13. Yuan JP, Zeng W, Huang GN, Worley PF, Muallem S (2007) STIM1 heteromultimerizes TRPC channels to determine their function as store-operated channels. *Nat Cell Biol* 9: 636–645.
14. Zhang SL, et al. (2008) Store-dependent and -independent modes regulating Ca^{2+} release-activated Ca^{2+} channel activity of human Orai1 and Orai3. *J Biol Chem* 283: 17662–17671.
15. Kawasaki T, Lange I, Feske S (2009) A minimal regulatory domain in the C terminus of STIM1 binds to and activates ORAI1 CRAC channels. *Biochem Biophys Res Commun* 385:49–54.
16. Muik M, et al. (2009) A cytosolic homomerization and a modulatory domain within STIM1 C terminus determine coupling to ORAI1 channels. *J Biol Chem* 284:8421–8426.
17. Park CY, et al. (2009) STIM1 clusters and activates CRAC channels via direct binding of a cytosolic domain to Orai1. *Cell* 136:876–890.
18. Yuan JP, et al. (2009) SOAR and the polybasic STIM1 domains gate and regulate Orai channels. *Nat Cell Biol* 11:337–343.
19. Zhou Y, et al. (2010) STIM1 gates the store-operated calcium channel ORAI1 in vitro. *Nat Struct Mol Biol* 17:112–116.
20. Mignen O, Thompson JL, Shuttleworth TJ (2008) Orai1 subunit stoichiometry of the mammalian CRAC channel pore. *J Physiol* 586:419–425.
21. Thompson JL, Mignen O, Shuttleworth TJ (2009) The Orai1 severe combined immune deficiency mutation and calcium release-activated Ca^{2+} channel function in the heterozygous condition. *J Biol Chem* 284:6620–6626.
22. Gwack Y, et al. (2007) Biochemical and functional characterization of Orai proteins. *J Biol Chem* 282:16232–16243.
23. Madl J, et al. (2010) Resting state Orai1 diffuses as homotetramer in the plasma membrane of live mammalian cells. *J Biol Chem* 285:41135–41142.
24. Ulbrich MH, Isacoff EY (2007) Subunit counting in membrane-bound proteins. *Nat Methods* 4:319–321.
25. Prakriya M, Lewis RS (2001) Potentiation and inhibition of Ca^{2+} release-activated Ca^{2+} channels by 2-aminoethyldiphenyl borate (2-APB) occurs independently of IP_3 receptors. *J Physiol* 536:3–19.
26. Yeromin AV, Roos J, Stauderman KA, Cahalan MD (2004) A store-operated calcium channel in *Drosophila* S2 cells. *J Gen Physiol* 123:167–182.
27. DeHaven WI, Smyth JT, Boyles RR, Bird GS, Putney JW, Jr. (2008) Complex actions of 2-aminoethyldiphenyl borate on store-operated calcium entry. *J Biol Chem* 283: 19265–19273.
28. Peinelt C, Lis A, Beck A, Fleig A, Penner R (2008) 2-Aminoethoxydiphenyl borate directly facilitates and indirectly inhibits STIM1-dependent gating of CRAC channels. *J Physiol* 586:3061–3073.
29. Zweifach A, Lewis RS (1993) Mitogen-regulated Ca^{2+} current of T lymphocytes is activated by depletion of intracellular Ca^{2+} stores. *Proc Natl Acad Sci USA* 90:6295–6299.
30. Mercer JC, et al. (2006) Large store-operated calcium selective currents due to co-expression of Orai1 or Orai2 with the intracellular calcium sensor, Stim1. *J Biol Chem* 281:24979–24990.
31. Peinelt C, et al. (2006) Amplification of CRAC current by STIM1 and CRACM1 (Orai1). *Nat Cell Biol* 8:771–773.
32. Ding H, Wong PT, Lee EL, Gafni A, Steel DG (2009) Determination of the oligomer size of amyloidogenic protein beta-amyloid(1-40) by single-molecule spectroscopy. *Biophys J* 97:912–921.
33. Xiao B, Coste B, Mathur J, Patapoutian A (2011) Temperature-dependent STIM1 activation induces Ca²+ influx and modulates gene expression. *Nat Chem Biol* 7: 351–358.
34. Tombola F, Ulbrich MH, Isacoff EY (2008) The voltage-gated proton channel Hv1 has two pores, each controlled by one voltage sensor. *Neuron* 58:546–556.
35. Xu P, et al. (2006) Aggregation of STIM1 underneath the plasma membrane induces clustering of Orai1. *Biochem Biophys Res Commun* 350:969–976.
36. Luik RM, Wu MM, Buchanan J, Lewis RS (2006) The elementary unit of store-operated Ca^{2+} entry: Local activation of CRAC channels by STIM1 at ER-plasma membrane junctions. *J Cell Biol* 174:815–825.
37. Li Z, et al. (2011) Graded activation of CRAC channel by binding of different numbers of STIM1 to Orai1 subunits. *Cell Res* 21:305–315.
38. Hoover PJ, Lewis RS (2011) Stoichiometric requirements for trapping and gating of Ca^{2+} release-activated Ca^{2+} (CRAC) channels by stromal interaction molecule 1 (STIM1). *Proc Natl Acad Sci USA* 108:13299–13304.
39. Fanger CM, Neben AL, Cahalan MD (2000) Differential Ca^{2+} influx, KCa channel activity, and Ca^{2+} clearance distinguish Th1 and Th2 lymphocytes. *J Immunol* 164: 1153–1160.
40. Demuro A, Parker I (2005) "Optical patch-clamping": Single-channel recording by imaging Ca^{2+} flux through individual muscle acetylcholine receptor channels. *J Gen Physiol* 126:179–192.